Electronic Supplementary Material (ESI) for ChemComm.

Supplementary Information

Nucleic-acids recognition interfaces: How the greater ability of RNA duplexes to bend towards the surface influences sensor performance

Roya Tavallaie,[a, b, c] Nadim Darwish,[a] D. Brynn Hibbert,[a] J. Justin Gooding* [a, b, c]

[a] School of Chemistry, The University of New South Wales, Sydney, NSW 2052, Australia.

[b] Australian Centre for NanoMedicine, The University of New South Wales, Sydney, NSW 2052, Australia.

[c] ARC Centre of Excellence in Convergent Bio-Nano Science and Technology, The University of New South Wales, Sydney, NSW 2052, Australia.

1. Experimental Details

1-1- Materials All DNA sequences were synthesized by either GeneWorks (Sydney, Australia) or Integrated DNA Technologies (Coralville, IA). The DNA sequences (probe sequences) had a C_6-thiol modification at either 3' or 5' end. The sequence information of the probes and targets are shown below and the mismatches in the targets are underlined.

DNA Probe: 5'-SH-$(CH_2)_3$-p-TCAACATCAGTCTGATAAGCTA-$(CH_2)_3$- MB-3'
RNA Probe: 5'-SH-$(CH_2)_3$-p-UCAACAUCAGUCUGAUAAGCUA-$(CH_2)_3$- MB-3'
DNA-Complementary: 5'-TAGCTTATCAGACTGATGTTGA-3'
RNA-Complementary: 5'-UAGCUUAUCAGACUGAUGUUGA-3'
DNA-Single Mismatch: 5'-TAGCTTATCAAACTGATGTTGA-3'
RNA-Single Mismatch: 5'-UAGCUUAUCAAACUGAUGUUGA-3'
DNA-Triple Mismatch: 5'-CAGCTTATCAAACTGATGTTGC-3'
RNA-Triple Mismatch: 5'-CAGCUUAUCAAACUGAUGUUGC-3'

6-Mercapto-1-hexanol (C_6OH) and components of buffer solutions including potassium phosphate dibasic, potassium phosphate monobasic, sodium chloride and magnesium chloride were from Sigma-Aldrich (Sydney, Australia).

1-2- Electrode Modification with Probe Nucleic acid and Hybridization Nucleic acid modified surfaces were prepared according to the classical method of Tarlov,[1] where thiolated DNA is bound to a gold surface and the DNA strands are spaced apart with a hydroxyl terminated alkanethiol diluent. A self-assembled monolayer (SAM) of probe nucleic acids was prepared by immersing clean gold electrodes in 4 μM solution of thiolated nucleic acid in phosphate buffered saline (PBS) for 2 h, followed by rinsing with Milli-Q water. The thiol groups chemisorb onto the gold surface *via* the formation of gold-thiol pseudo covalent bond to produce the nucleic acid monolayer. The probe nucleic acid modified gold electrodes were rinsed with PBS prior to adsorption of a diluent layer. The diluent layer of alkanethiol molecules terminated with alcohol moieties was further self-assembled onto the probe nucleic acid layer by immersing them in 2 mM 6-mercaptohexanol solution for 30 minutes, followed by rinsing with PBS. Hybridization of target nucleic acid was performed at room temperature by immersing the probe nucleic acid/diluent modified gold electrodes in 4 μM solutions of target (unless stated otherwise) in PBS containing 5 mM $MgCl_2$ for 2 h, followed by rinsing with PBS.

1-3- Quantification of the Amount of Redox Labelled Probe Nucleic Acids Immobilized on the Electrode The density of electroactive redox labelled DNA/RNA probes on the electrode surface was determined by integrating the area under the methylene blue reduction peak in the CVs using the **Equation 1**.

$$\Gamma = \frac{Q}{nFA} \qquad \textbf{Equation 1}$$

where Q is the integration of charges under the oxidation peak, n is the number of electrons transferred per redox event (n = 2), F is the Faraday constant, and the A is the electrode area.

1-4- Instrumentation and Procedure Square wave voltammetry (SWV), cyclic voltammetry (CV) experiments were performed in a cell made of glass using BAS 100B potentiostat (Bioanalytical Systems, Inc.). An Ag/AgCl (3M KCl) was the reference electrode and a

platinum wire was the auxiliary electrode. The immobilization buffer solution (PBS) was used as the electrolyte. The solution was degassed with argon for at least 15 min before data acquisition. The SWV measurement was performed at pulse amplitude of 25 mV, step of 4 mV, and frequency of 10 Hz. Electrochemical impedance spectroscopy measurements were performed using Solartron 1287 potentiostat (Farnborough) at the frequency range of 0.1 to 100000 HZ and potential of -0.275 V.

2. Results

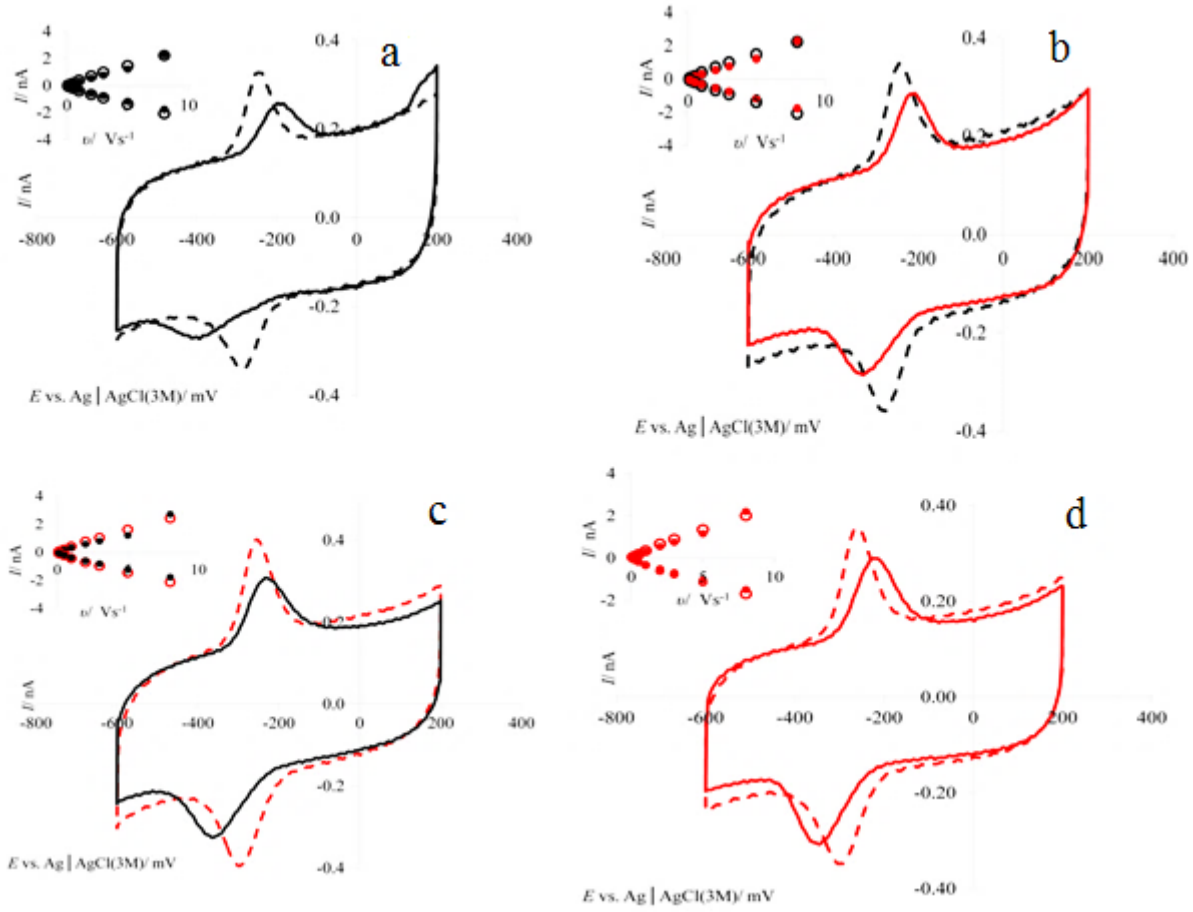

Fig. S1 Cyclic voltammograms recorded with the probe DNA (black) and RNA (red) modified electrodes before (dashed line) and after (solid line) hybridization with target DNA and RNA. Scan rate was 1 V s^{-1}. The inset of figures represents the dependence of cathodic current to the scan rate before (no fill) and after (filled dots) hybridization. a: MB-DNA/DNA, b: MB-DNA/RNA, c: MB-RNA/DNA, d: MB-RNA/RNA. Peak to peak separation (ΔE_p) was 158, 77, 84 and 88 mV for MB-DNA/DNA, MB-DNA/RNA, MB-RNA/RNA and MB-RNA/DNA systems, respectively. Comparing the ΔE_p values obtained for the studied systems, the same order (MB-DNA/DNA> MB-RNA/DNA> MB-RNA/RNA> MB-DNA/RNA) was observed at higher scan rates.

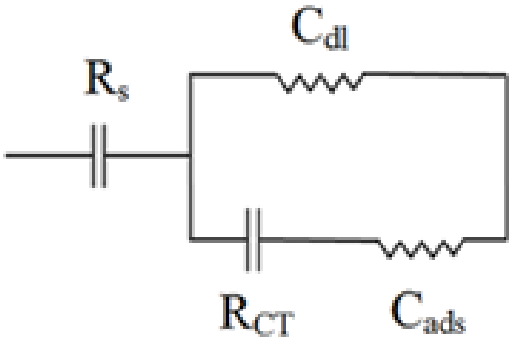

Fig. S2 The equivalent circuit used to fit the experimental data is shown. Impedance data were interpreted by fitting the data to equivalent circuit model using the complex non-linear least-squares (CNLS) technique included in the frequency-response analysis software.[2] In the model, the R_s is the solution or electrolyte resistance, R_{CT} represents the charge transfer resistance. Here the true double layer capacitance (C_{dl}) is replaced by a constant phase element (C_{PE1}) and Warburg impedance (Z_w) replaced by another constant phase element (C_{PE2} or capacitance of the adsorbed molecules).[3] The value of the parameters which has been obtained from the fitting of data together with the estimated apparent rate constant for electron transfer for each system before and after hybridization is listed in Tables 1S.

Table S1 EIS fitting analysis results for each system.

	R_s/ Ω	CPE_{dl}-T/ F	R_{CT}/ Ω	CPE_{ads}-T/ F	k_{EIS}
MB-DNA	277.0 (3.60)	2.19E-07 (2.19E-09)	95032 (1045.35)	1.68E-07 (5.71E-10)	62.64 (0.9)
MB-RNA	253.5 (2.78)	2.18E-07 (2.09E-09)	59382 (1039.18)	2.59E-07 (2.15E-09)	65.07 (1.67)
MB-DNA/$DNA_{Complementary}$	267.7 (2.54)	1.43E-07 (1.26E-09)	929470 (8876.43)	1.98E-07 (1.41E-09)	5.43 (0.09)
MB-DNA/DNA_{MM1}	271.3 (4.61)	1.37E-07 (1.32E-09)	561470 (10667.93)	2.25E-07 (2.23E-09)	7.92 (0.22)
MB-DNA/DNA_{MM3}	263.3 (5.79)	2.08E-07 (2.50E-09)	90506 (2805.686)	2.20E-07 (1.21E-09)	50.22 (1.83)
MB-DNA/$RNA_{Complementary}$	329.2 (3.29)	1.27E-07 (9.49E-09)	462500 (9712.5)	1.60E-07 (1.39E-09)	13.55 (0.40)
MB-DNA/RNA_{MM1}	310.7 (2.64)	1.71E-07 (1.59E-09)	249140 (2491.4)	1.13E-07 (7.32E-10)	35.64 (0.58)
MB-DNA/RNA_{MM3}	290.1 (7.54)	2.00E-07 (3.40E-09)	159590 (1372.47)	1.49E-07 (1.10E-09)	42.05 (0.67)
MB-RNA/$DNA_{Complementary}$	163.9 (1.31)	1.43E-07 (1.36E-09)	405240 (8915.28)	2.82E-07 (2.82E-09)	8.75 (0.28)
MB-RNA/DNA_{MM1}	309.5 (4.33)	1.41E-07 (1.97E-09)	399830 (3558.48)	1.53E-07 (1.48E-09)	16.32 (0.30)
MB-RNA/DNA_{MM3}	310.7 (5.90)	1.71E-07 (1.42E-09)	249140 (3986.24)	1.13E-07 (6.22E-10)	35.52 (0.76)
MB-RNA/$RNA_{Complementary}$	263 (3.55)	1.40E-07 (1.22E-09)	348480 (5575.68)	2.85E-07 (3.02E-09)	10.07(1.22)
MB-RNA/RNA_{MM1}	309.5 (2.75)	1.41E-07 (1.35E-09)	399830 (3198.64)	1.53E-07 (1.30E-09)	16.35 (0.27)
MB-RNA/RNA_{MM3}	420.9 (8.37)	3.20E-07 (8.00E-09)	193380 (5801.4)	1.13E-07 (2.49E-10)	45.76 (1.47)

The relationship between the circuit elements (C_{dl}, double-layer capacitance; C_{ads}, adsorption pseudo-capacitance; R_{CT}, charge-transfer resistance) of the model presented at Fig. 2S and the parameters characterizing a redox system of strongly adsorbed electroactive species has been previously described,[3, 4] and the electron-transfer rate can be simply expressed as $k = (2R_{CT}C_{ads})^{-1}$. We remark that both C_{dl} and C_{ads} did show a frequency-dependent capacitive behavior and were therefore treated as constant-phase elements (CPEs) for which the impedance is equal to $C(j\omega)^{\varphi}$, in which C is the capacitance, ω is the angular frequency, and φ is an exponential term with a value between 0 and 1, where 1.0 is an ideal capacitor. Using the refined R_{CT} and C_{ads} values, the apparent ET rate constant (k) were calculated. The values in brackets are the estimated error obtained from the fitting.

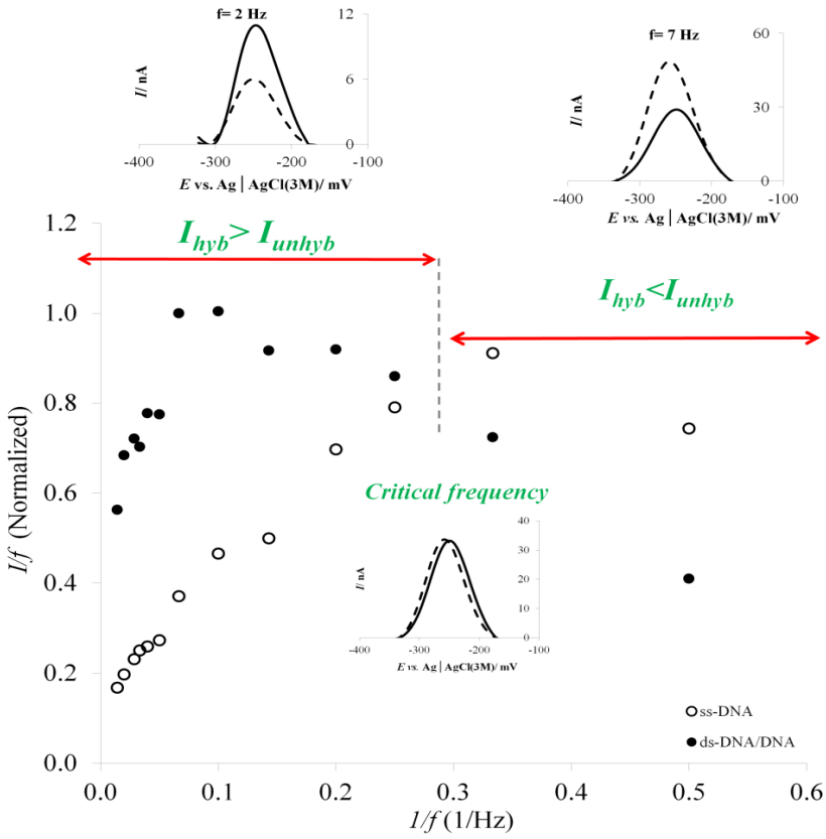

Fig. S3 illustrates a representative example of the frequency dependent hybridization induced change in the SWV current of the surfaces modified with MB labelled probe nucleic acids (in this example probe DNA) before(no fill) and after (black fill) hybridization with target (in this example target DNA). Comparing the SWV current before(dashed line) and after (solid line) hybridization, the unhybridized probe with the relatively faster electron transfer rate, shows the lowest relative current compared to that of after hybridization, when electron transfer is relatively slower, at low frequencies. However, as the frequency increases, the current from the unhybridized probe, with the faster electron transfer rate, increases and eventually become equal to that of the hybridized one at higher frequencies before exceeding that of the hybridized case. This frequency, in which the hybridization induced change in the SWV current approaches zero, will be referred to as the cross-over frequency. Finally, current from the unhybridized probe becomes larger than the hybridized probe at frequencies above the cross-over frequency. Indeed, this trend, which is reported previously for MB-DNA/DNA system,[5] demonstrates the signal-on discrimination of the unhybridized against the hybridized probes at frequencies below the cross-over frequency in contrast to the signal-off type at frequencies above the cross-over frequency. These variations in the hybridization induced change in the SWV current with frequency is a result of specific current sampling method used in the SWV technique. Considering the sampling points in the SWV at the end of each potential pulse, the observed current will behave very differently depending on whether the electron transfer reaction is rapid or slow relative to the frequency of the square wave pulse. In the case of a long pulse at low frequency, a faster electron transfer reaction (unhybridized probe) will already be completed by the sampling time, while slower one (probe after hybridization) will still show a response. However, a short pulse at relatively higher frequencies will result in the higher currents for the faster electron transfer reaction (probe before hybridization) while the slower one (before hybridization) cannot keep pace with the rapidly changing potential (the potential is reversed before the ET reaction is finished and before the current response reaches the maximum at the begining of the reverse potential pulse) and thus contribute less to the square wave current.

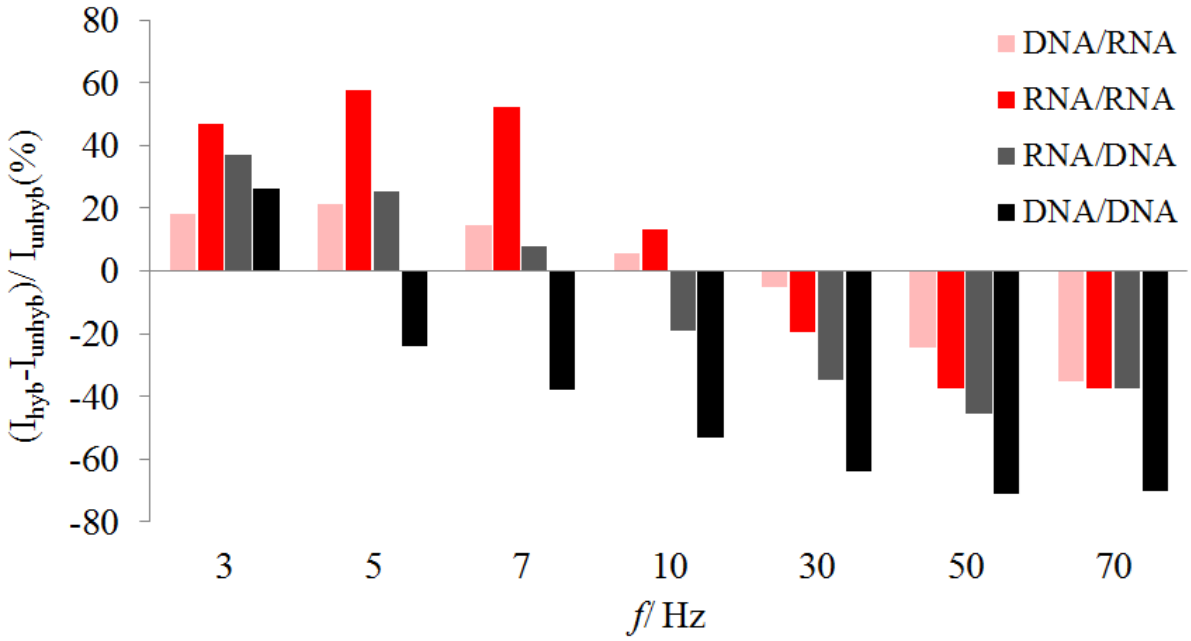

Fig. S4 compares the hybridization induced changes in the SWV current at different frequencies in four studied systems. It could be observed that the MB-DNA/RNA, MB-RNA/RNA and MB-RNA/DNA systems follow a similar trend of frequency-dependent hybridization induced change in the SWV current as was observed in the MB-DNA/DNA system. However, the cross-over frequency, in which the systems are switching to signal-off behavior, together with the extent by which current is changing after hybridization, is different for each system under the experimental conditions of 25 mV amplitude, 22° C. The cross-over frequency was found to be at 5, 7, 10 and 15 Hz for MB-DNA/DNA, MB-RNA/DNA, MB-RNA/RNA and MB-DNA/RNA systems, respectively. The pulse frequency is a time function. Therefore a shift in the cross-over frequency to higher frequencies in MB-RNA/DNA, MB-RNA/RNA and MB-DNA/RNA systems, compared with the MB-DNA/DNA system, reflects the different time scales for the dynamics of double helix bending such that the redox label can access the electrode surface. The difference in the position of cross-over frequency could be used to discriminate four systems from each other by synchronizing the pulse potential frequency in the SWV. Comparing the hybridization induced change in current after hybridization with RNA, it could be seen that at frequencies below the cross-over frequency MB-RNA/RNA system shows higher change in the current after hybridization, compared to the MB-DNA/RNA system. However, by increasing the frequency both systems tend to reach to almost the same level of change in the current.

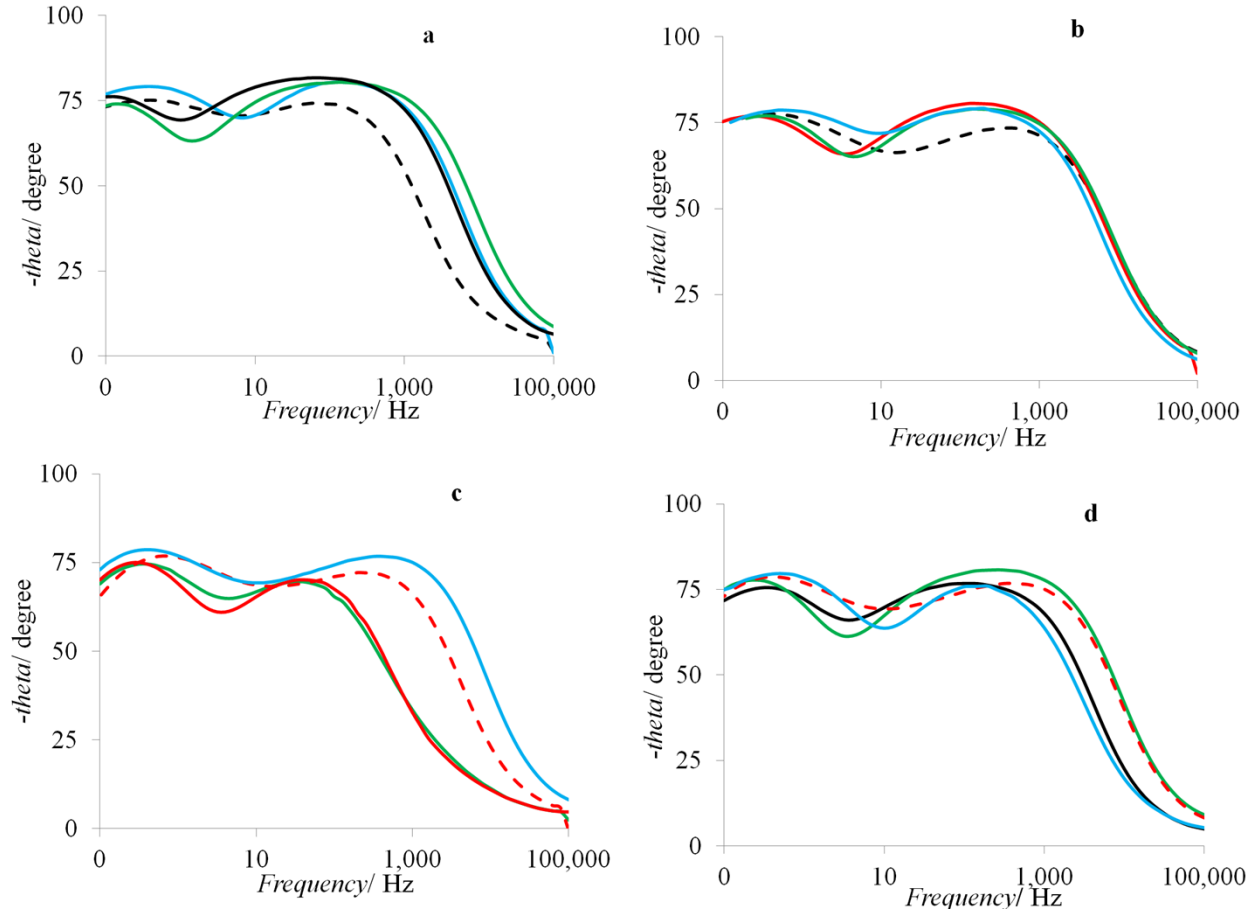

Fig. S5 Comparative Bode plots obtained before (dashed line) and after hybridization (solid) with target DNA(black)/ RNA(red), single (green) and triple (blue) mismatch base pairs in same experimental conditions. a: MB-DNA/DNA, b: MB-DNA/RNA, c: MB-RNA/RNA, d: MB-RNA/DNA

References

1. K. A. Peterlinz, R. M. Georgiadis, T. M. Herne and M. J. Tarlov, *J. Am. Chem. Soc.*, 1997, **119**, 3401-3402.
2. J. R. Macdonald and L. D. Potter, *Solid State Ionics*, 1987, **24**, 61-79.
3. S. E. Creager and T. T. Wooster, *Anal. Chem.*, 1998, **70**, 4257-4263.
4. A. D. Abhayawardhana and T. C. Sutherland, *J. Phys. Chem. C*, 2009, **113**, 4915-4924.
5. R. J. White and K. W. Plaxco, *Anal. Chem.*, 2010, **82**, 73-76.